The 2012 World Congress on
Advances in Civil, Environmental, and Materials Research (ACEM' 12)
Seoul, Korea, August 26-30, 2012

Synthesis and Characterization of FeO-ZrO_2 Nanoparticles for Bio-medical Applications

Saher Hamid[1)], Saira Riaz[1,2)*], and Shahzad Naseem[2)]

[1), 2)] *Centre of Excellence in Solid State Physics, Punjab University, Lahore 54590, Pakistan*
[2)] saira_cssp@yahoo.com

ABSTRACT

Present work is an appraisal of the effectiveness of FeO in the stabilization of tetragonal zirconia (ZrO_2) nanoparticles synthesized under different conditions for bio-medical especially dental applications. Zirconia based ceramics have found broad biomedical applications because of their unusual combination of strength, fracture toughness, hardness, and low thermal conductivity. These attractive characteristics are largely associated with the stabilization of tetragonal and cubic phases through alloying with aliovalent ions. The high fracture toughness exhibited by many of zirconia ceramics is attributed to the tetragonal to monoclinic phase transformation and its release during crack propagation. Objectives of the present work include preparation of α-Fe_2O_3 doped and un-doped ZrO_2 nano-powders by sol-gel method. This work also includes thin film growth of zirconia nanoparticles with a thickness of 100 nm by spinning the sol onto glass substrates. Temperature, pH, nature of solvent and synthesis conditions played critical role in the size reduction of these zirconia nanoparticles. X-ray diffraction (XRD) results show formation of tetragonal phase at 300°C when sample was heated for 60 minutes. Calcined powders at 500ºC exhibited crystallite size as low as 11 nm as revealed by XRD results, whereas grain size ~30 nm was observed by scanning electron microscopy (SEM). Vickers Hardness measurements showed ~564 HV hardness of ZrO_2 samples prepared by sol-gel. Thus, sol-gel has proven to be a low cost, reliable and application oriented technique for the preparation of nanoparticles.

1. INTRODUCTION

The improvement of zirconia (ZrO_2) nanoparticles has attained much attention because of their multifunctional properties (Dwivedi 2011). It has been stated that the main crystal phases of ZrO_2 are cubic, tetragonal and monoclinic and the main IR frequencies are 480, 435 and 270 cm^{-1} for cubic, tetragonal and monoclinic phases, respectively (Chuach 1996, Chuach 1999). It shows that host ZrO_2 has different phonon energy for different crystal phases. The monoclinic phase of zirconia is stable from room temperature up till 1100 °C, while the tetragonal phase of zirconia is stable between ranges of 1100 °C to 2370 °C. When the temperature increases above 2370°C it is observed that the cubic form of zirconia appears which is stable for all higher temperatures (Dwivedi 2011). Zirconia has a wide number of applications such as, in bio-sensors, solid oxide fuel cells, oxygen sensors, H_2 gas storage materials, catalyst and catalyst support (Chuach 1999, Chuach 1996, Minh 1993, Martinson 2007). In

accumulation zirconia is a material which could also be used as dielectric material, electro-optic material, and piezoelectric material (Kim 2001, Laurent 2001). For dissimilar catalytic applications, zirconia is also used as maintenance material to disperse several noble and transition metals.

Zirconia is stated as an n-type semiconductor material with good electrical properties (Reddy 2005). It is also a famous solid acid catalyst. ZrO_2 is used as toughening ceramic (Ramalingam 2011) in thighbone and oral planting (Prabakaran 2005, Chevalier 2009). It has also been stated freshly that oxides of nanoparticles have good applications in the field of photonics but a suitable contact with the adjacent medium is required (Majchrowski 2009).

Generally, at room temperature the tetragonal phase of pure zirconia can never be reversed by quenching for the reason that of the diffusion-less martensitic transition into monoclinic zirconia (Jiang 1998). By doing a wide research (Bastide 1989) on the phase stability of zirconia, it has been proved that by the addition of various main groups, lanthanide or transition metals, stabilized zirconia (S-ZrO_2) can be molded at room temperature even though the exact mechanism of stabilization remains unclear. The stabilization of high temperature phases of zirconia i.e. tetragonal phase or cubic phase is possible if zirconia structure is familiarized by appropriate aliovalent cations such as Mg^{2+} , $Ca^{2+,}$ Gd^{3+}, Y^{3+} and also with some of the rare earth cations form solid solutions with zirconia, thus stabilizing the tetragonal or cubic phase with increasing contents. Stabilized form of zirconia has a large number of biomedical, electronic, chemical, and mechanical applications (Ausheliba 2012). High temperature phases of zirconia can also be stabilized when iron cations (Fe^{3+}) alloy with zirconia, but the use of undersized dopants (for example Ga^{2+} or Fe^{3+}) leads to a less efficient stabilization of zirconia. It is proposed by Stefanic et al (Stefanic 2000) that the amalgamation of iron into zirconia has both stabilizing and destabilizing influence on the high temperature phases of zirconia, as a function of air pressure used for the calcination.

The influence of iron ions has not been very much studied as a stabilizer. It has been stated (Boutz 1994) that when minor quantities of hematite (α-Fe_2O_3) are added to zirconia in order to stabilize the zirconia phases, it leads firstly to deprivation of destabilizing the tetragonal phase of zirconia to a significant growth in the density during sintering and then secondly towards a growth of creep rate by a factor of 4 to 6 (Garcia 2009). In the tetragonal structure of zirconia the amalgamation of iron ions stabilizes the cubic phase of zirconia and consequently prevents its transformation to the monoclinic phase. It was reported by Kiminami et al that the small accompaniments (>1 Mol%) of iron into the zirconia structure upsurge the hysteresis gap of the monoclinic-tetragonal alteration (Kiminami 1999). It has been stated that the methods used for synthesis has a very strong impact on the degree of amalgamation of iron ions (Asghar 2010), into the monoclinic, tetragonal and the cubic zirconia lattices.

In this present work, a sol-gel method was used for the synthesis of iron doped zirconia, which consequently forms a solid solution that has a minimal concentration 0.02 Mol% Fe_2O_3-ZrO_2 and development of this solution with different annealing treatments at raised temperatures have been examined. Effect of organic additives such as glucose and fructose, on the shape and size of nanoparticles, has also been studied. They are actually acting as capping agents and are able to inhibit particles from their

agglomeration, which results in the decrease of particle size so that the transformation of phase from tetragonal to monoclinic can be prohibited (Heshmatpour 2011).

2. EXPERIEMENT

2.1 Materials

High purity chemicals zirconium oxychloride ($ZrOCl_2 \cdot 8H_2O$), N-propanol, glucose, fructose and aqueous Ammonia (25%) were used as precursor, solvent and organic agents respectively. 0.02 M% iron oxide (α-Fe_2O_3) was used to prepare iron oxide doped ZrO_2 nanoparticles. Zirconium oxychloride has been used as zirconium salt, which is comparatively cheaper than other salts of zirconium i.e. zirconium chloride, zirconium oxynitrate hydrate and zirconium nitrate.

2.2 Synthesis of Un-doped and α-Fe_2O_3 doped ZrO_2 nanopowder

In the beginning, 0.3 g zirconium oxychloride ($ZrOCl_2.8H_2O$) was added to10ml n-propanol. Then, by a drop by drop addition of ammonia and distilled water the ensuing solution was hydrolyzed to attain a pH value of 9. For the process of hydrolysis, a volume ratio of 1:4 of zirconium salt to water was used. Two organic additives, glucose and fructose were used since these are cheaper, nontoxic, and easily accessible at a low temperature to store; they are effectively supplied and are water soluble. The benefits of using sol-gel method are that it is environmentally friendly and this method takes only 15 to 20 hours in aggregate. A mixture of glucose and fructose was prepared with a mass ratio of 1:1 and added to the solution under vigorous stirring. Continued stirring was applied until a homogenous solution was obtained. After the homogenization, the solution was stirred at a temperature of 50 ^oC for 3 hours so that the resulting gel was polymerized. For the doping purposes 0.02M% iron oxide sol was prepared by sol-gel route reported earlier by our group (Riaz 2012). Fe_2O_3 sol was then added drop wise to the ZrO_2 sol and stirred for 3 hours to obtain a homogenous iron oxide doped ZrO_2 sol. Fig. 1 illustrates the steps of procedure.

In order to dehydrate the gel, an oven was used at a temperature of 110^oC for 3 hours. Thus, at several temperatures in between the ranges of 110 to 450^oC all the samples, doped and un-doped, went through a calcination treatment in a furnace for 1 to 3 hours.

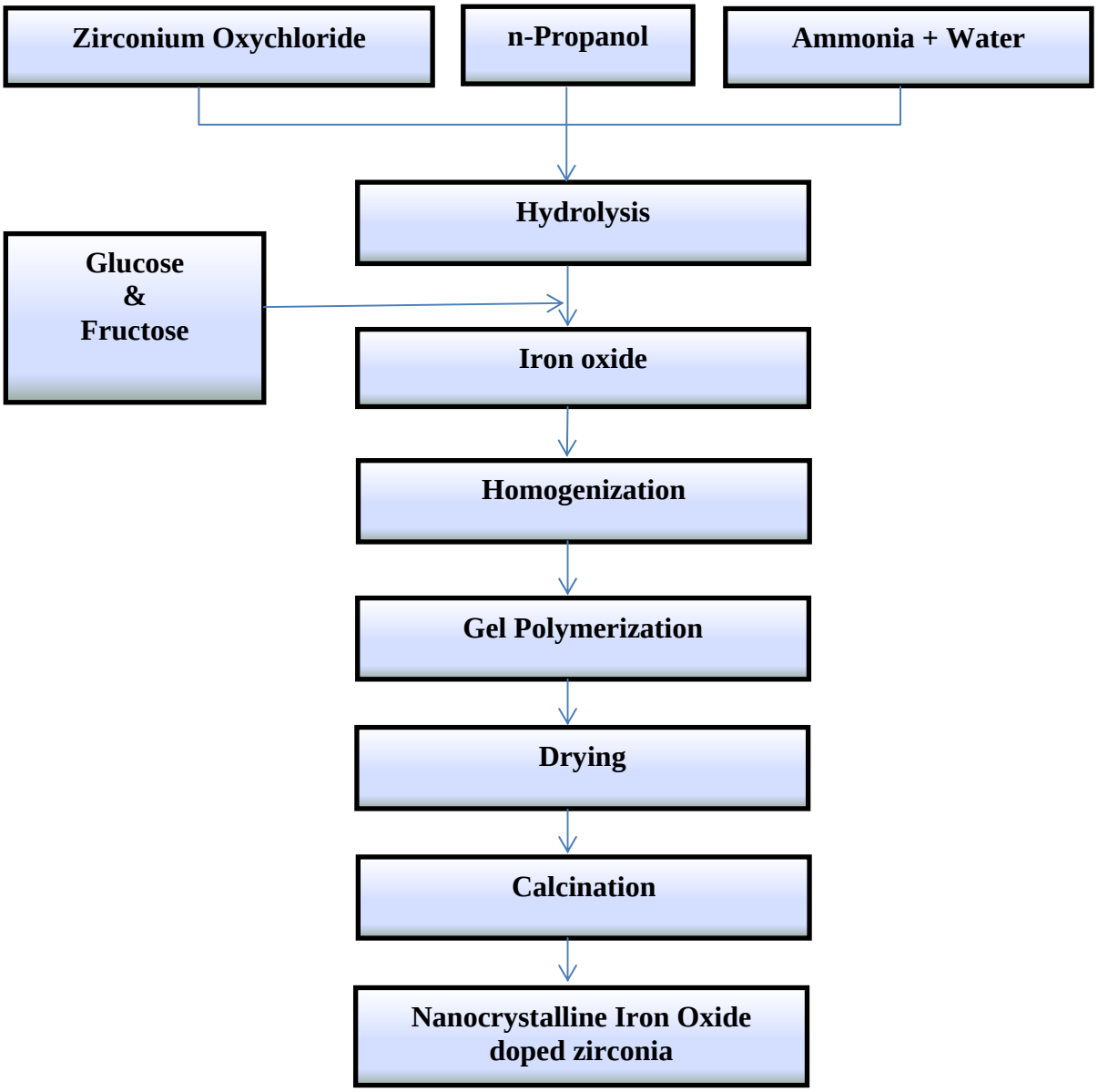

Fig. 1 Step by step procedure for the synthesis of α-Fe_2O_3 doped ZrO_2 nanoparticles by sol–gel method.

2.3 Characterization:

The prepared zirconia nanoparticles were inspected by powder X-ray diffraction, using CuKα radiation (λ=1.5405Å), Rigaku D-MAX/IIA X-ray diffractometer, to confirm the phase and structure. The morphology and size of the zirconia nanoparticles were examined by scanning electron microscopy (SEM). SEM images were attained using Hitachi S-3400N scanning electron microscope at accelerating voltage of 30 kV. Bruker CP-II Atomic Force Microscopy (AFM) was used for surface topology and grain size of the particles. Shimadzu Vicker's hardness tester was used to measure hardness of the samples.

3. RESULTS AND DISCUSSIONS

Fig. 2 shows the XRD patterns of un-doped zirconia annealed at different temperatures. Appearance of characteristic ZrO_2 (111) peak at 29.9^o confirms the crystalline structure of zirconia. The tetragonal phase formation of the zirconia starts when the elimination of OH ions occurred by increasing the annealing / calcination temperature of the samples. In Fig.2 other distinguished ZrO_2 peaks indicate the presence of (200), and (202) planes. Appearance of all these planes confirms the tetragonal phase of zirconia when compared with the JCPDS card no 17-923. Tetragonal phase of ZrO_2 is basic requirement for their application in the bio-medical fields especially in oral planting (Manicone 2007).

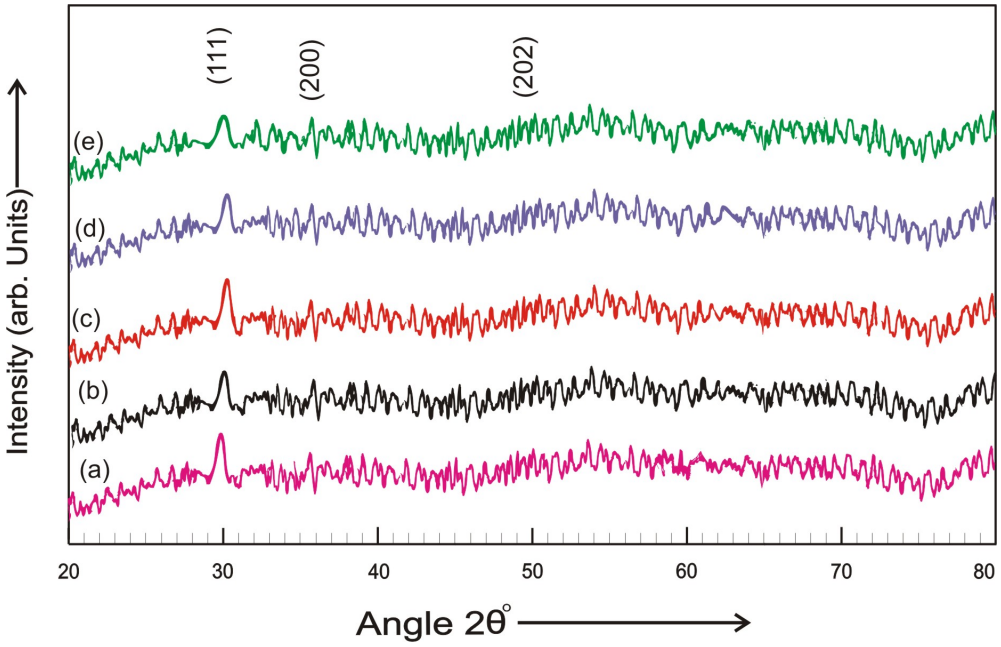

Fig. 2 XRD results of un-doped zirconia

Full Width Half Maximum (FWHM) of (111) was found to be 0.371^o at 110 ^{o}C. The variation of FWHM of (111) is plotted in Fig. 3. Broadness appears in the peaks as can

be seen in Fig. 2 as well. This broadness in the peaks shows an increase in FWHM which correspondingly gives a small crystalline size.

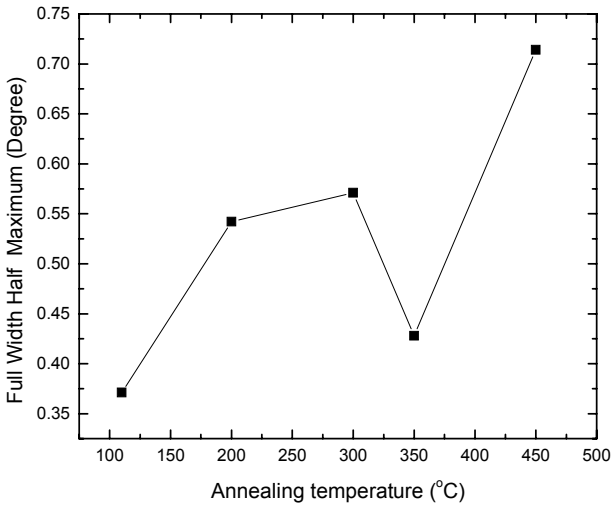

Fig. 3 Variation in FWHM ZrO_2 (111) plane

Lattice parameters were calculated by using the relation given in Eq. (1):

$$1/d^2 = (h^2 + k^2)/a^2 + l^2/c^2 \qquad (1)$$

The values obtained (a = 5.18 Å, c=5.30 Å) are in close agreement with the standard values of lattice parameters.

In order to determine the crystallite size of each sample annealed at dissimilar temperatures, Debye Scherrer formula, given in Eq. (2), was used.

$$t = k\lambda/B\cos\theta \qquad (2)$$

Where, k = 0.9 stands for shape factor, (λ=1.5405Å) represents the wavelength of Cukα radiation, half width of each diffraction peak is denoted by B, t stands for the crystallite size of particles.

Whereas, the microstrain developed inside the nanoparticles was calculated by using the expression given in Eq. 3.

$$\Delta d/d = \qquad (3)$$

Fig. 4 shows effect of calcination temperature on the resultant particle size and stress/strain calculated from XRD patterns. Calculated values of strain and particle size for each of the sample are also mentioned in Table 1.

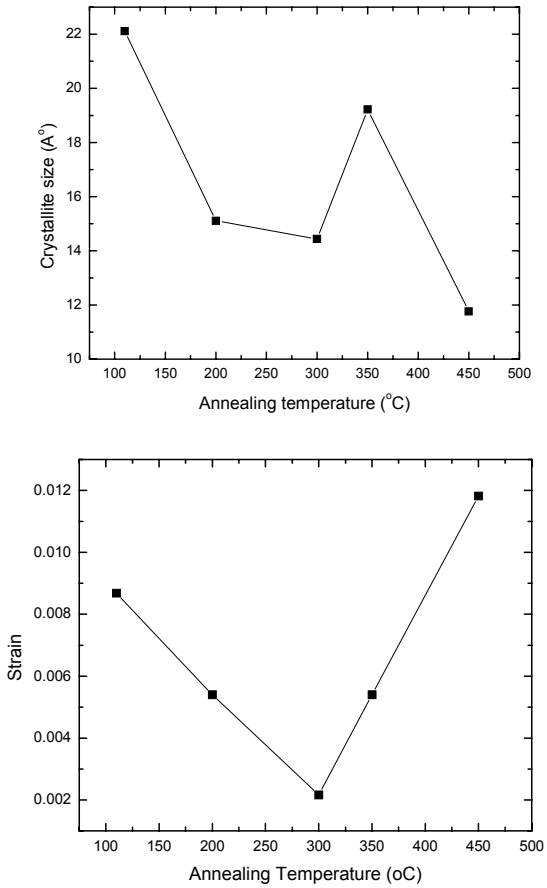

Fig. 4 Variation in (a) particle size and (b) Microstrain in ZrO_2 nanoparticles obtained from XRD pattern

It can be seen from Fig. 4(a) that overall a decreasing trend in particle size values was observed. However, a small increase in the temperature range of 300 – 350^{o}C was observed. This might be due to the reason that by increasing the annealing temperature the OH ions, which are one of the main species to affect and control the particle size, is eliminated. This elimination results in the appearance of tetragonal ZrO_2 phase. It is also observed that, as annealing temperature is increased the crystallinity of zirconia also increases. Similarly the planes (200) and (202) also confirm the tetragonal phases of zirconia.

Table I: XRD results of un-doped zirconia, represents the crystallite sizes, FWHM, Strain corresponding to annealing temperature.

Sample	Organic Additives	Annealing Temperature (^{o}C)	FWHM	Particle Size (nm)	Strain (Δd/d)
A	No	110	0.371	22.11	0.00868
B	No	200	0.542	15.11	0.00540
C	Yes	300	0.571	14.44	0.00216
D	Yes	350	0.428	19.22	0.00540
E	Yes	450	0.714	11.76	0.01182

Scanning electron micrographs of un-doped zirconia are shown in Fig. 5, which shows ZrO_2 nanoparticles without addition of organic additive and Fig. 5 (d-f) with the addition of organic additive. The tetragonal crystallites of ZrO_2 within an aggregate underwent grain growth during the calcination treatment are presented in the SEM images. Material's agglomeration in the form of curling grain-like structure can be seen in Fig. 5(a) at low annealing temperature. However, when the temperature was increased beyond 300˚C very fine spherically shaped nanoparticles are observed. When the additive was used in preparation of ZrO_2 nanoparticles uniformity in the size and shape of nanoparticles is observed. It shows that there is a direct relation between the organic additives and the uniformity of the particle size. It could also be observed that the particle size also reduces by using organic additives. Without the use of organic additive particle sizes are in the range of 40-50nm, while with the use of organic additives the particles sizes reduces to 30-35nm.

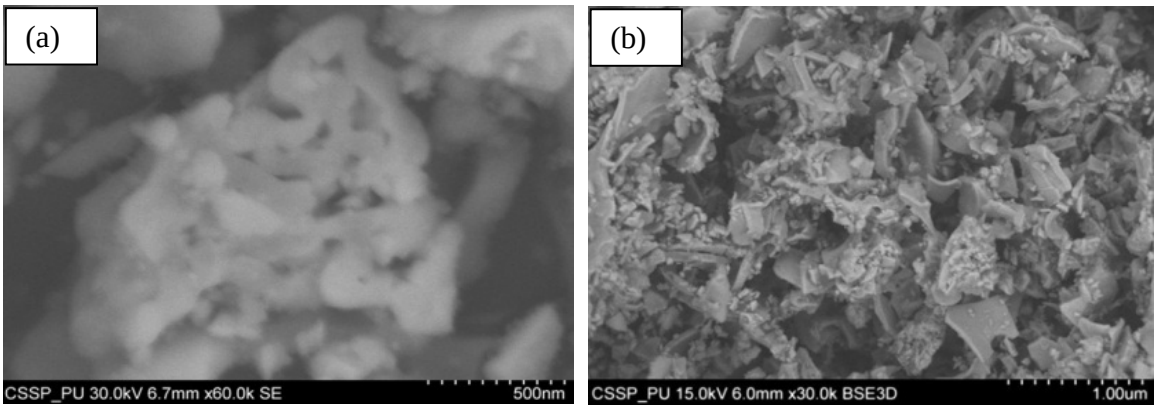

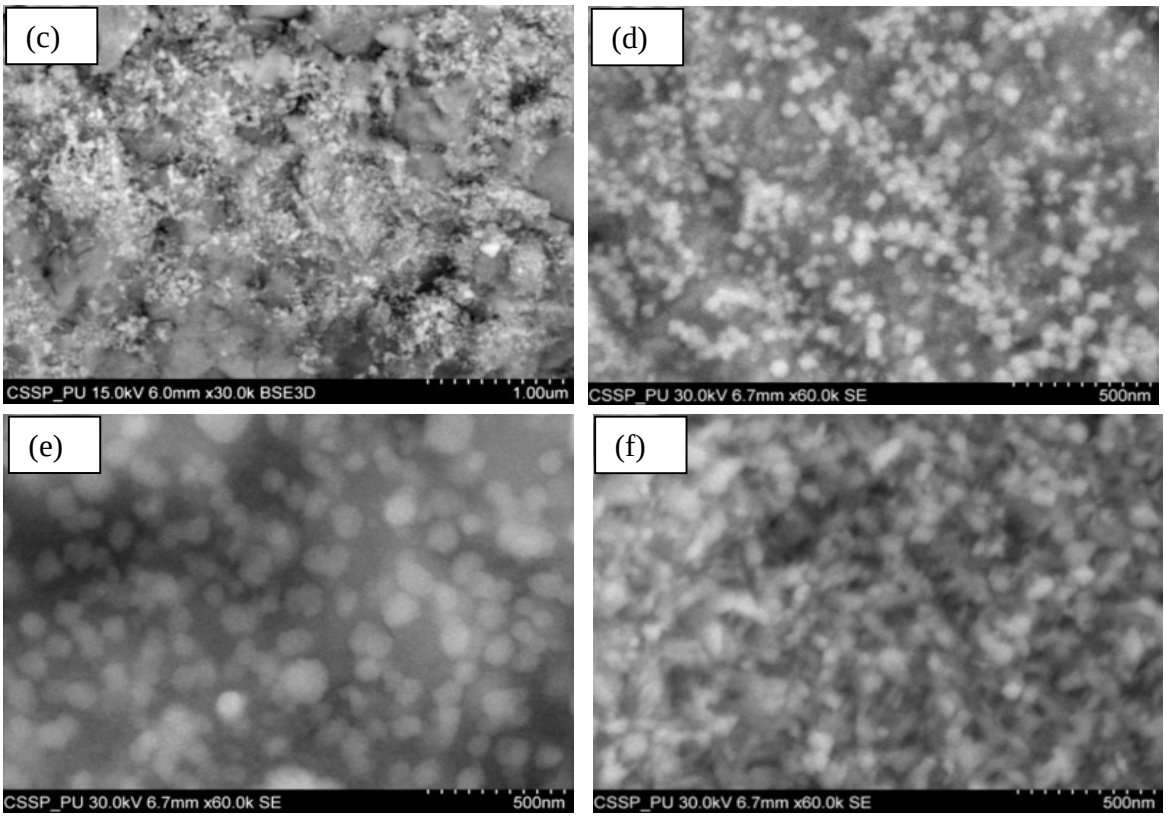

Fig. 5 SEM micrographs of undoped of zirconia samples

Fig. 5 shows the result obtained from FeO- doped ZrO_2 sample annealed at 300 ^oC for 2hours. It is observed that amorphous materials were found in the FeO-ZrO_2 catalyst, which shows that either any calcination treatment is given 100% crystallinity in material cannot be achieved (Ortiz 2010). It is also observed from the Fig. 5 that different morphologies were adopted by the doping material when it is compared to un-doped micrographs of SEM, and triggered dissimilar crystal phases during the annealing process of the doped samples. The doping agent shows that there is a less agglomeration of particles. The SEM micrograph of FeO-ZrO_2 shows a particle size distribution in the range of ~30–35nm. The FeO-ZrO_2 sample offered nanoparticles with more consistent quasi spherical shapes as compared to fig.4 (d and e), which may be due to the presence of oxides of Iron. However, there is no any significant effect on the size of these nanoparticles as compared to the size observed in organic based ZrO2 nanoparticles i.e. ~ 30 – 35nm.

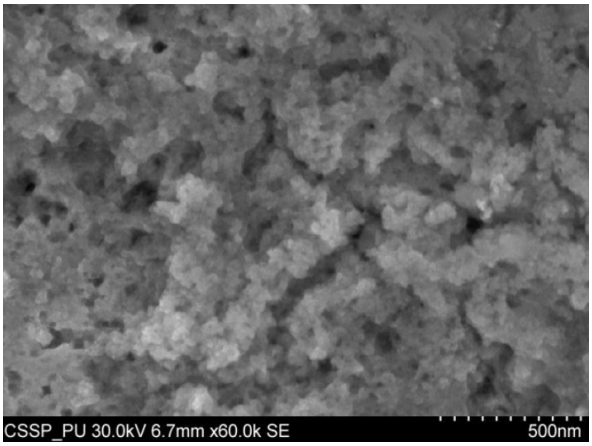

Fig. 6 SEM micrographs of doped of zirconia sample

3.3 Atomic Force Microscopy (AFM) analysis:

Fig.7 (a-e) shows the results obtained from 2D and 3D Atomic Force Microscopy (AFM) images along with area analysis of zirconia nanopowder without the use of any doping agent. AFM gives the information about surface topography of the samples. The results obtained from the AFM are shown in Table II and plotted in Fig. 8 (a-b) below:

(a)

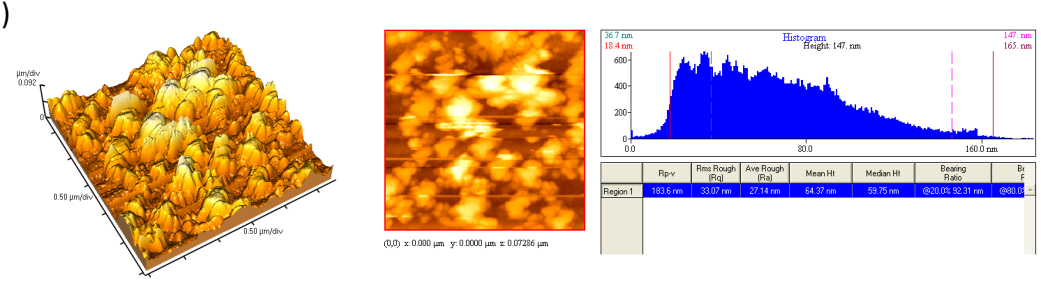

(b)

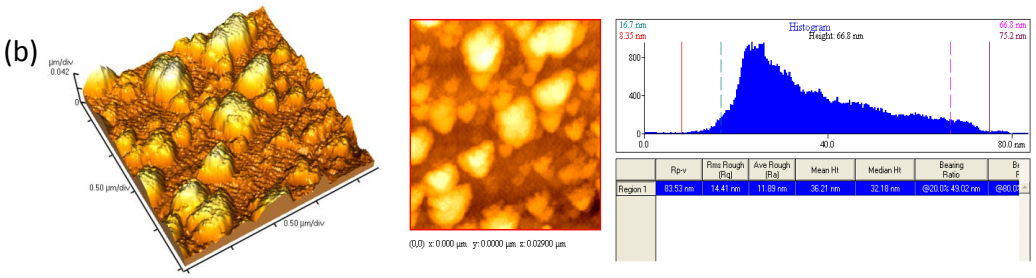

(c)

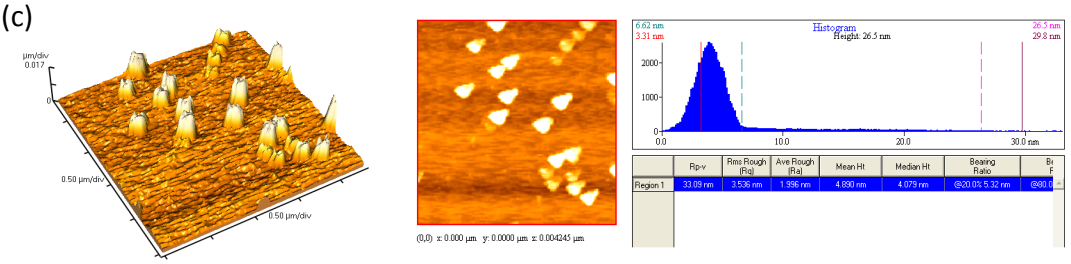

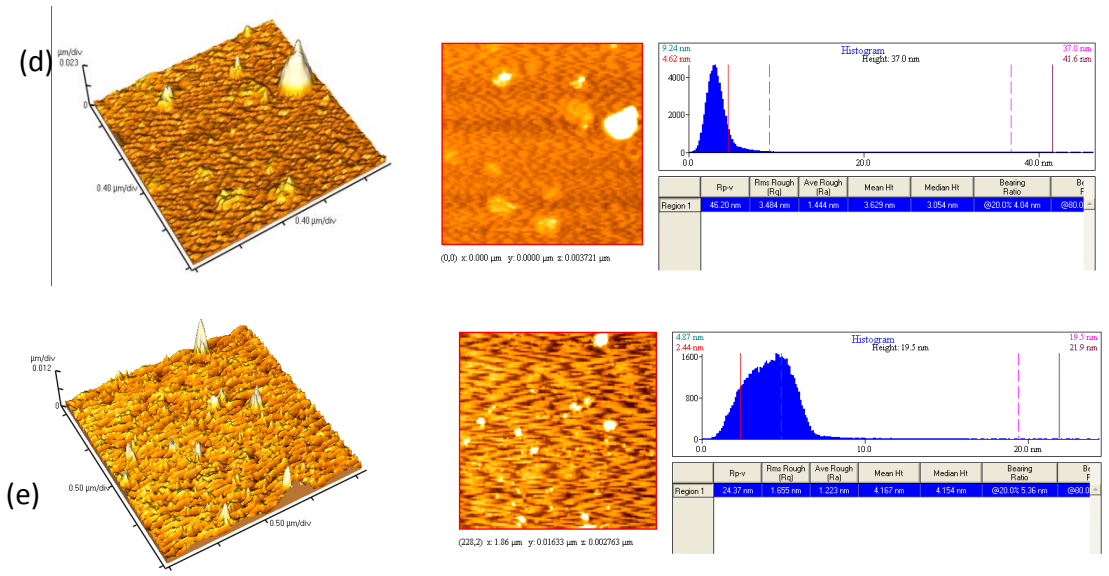

Fig. 7 (a-e) AFM images of un-doped zirconia

Table II: AFM results of un-doped zirconia

Sample	Organic Additives	Annealing Temperature (^oC)	Average Rough (nm)	Rms Rough (nm)	Median Ht (nm)	Mean Ht (nm)
A	No	110	27.14	33.07	59.75	64.37
B	No	200	11.89	14.49	4.079	4.890
C	Yes	300	1.996	3.536	3.054	3.629
D	Yes	350	1.444	3.484	32.18	36.21
E	Yes	450	1.223	1.655	4.154	4.167

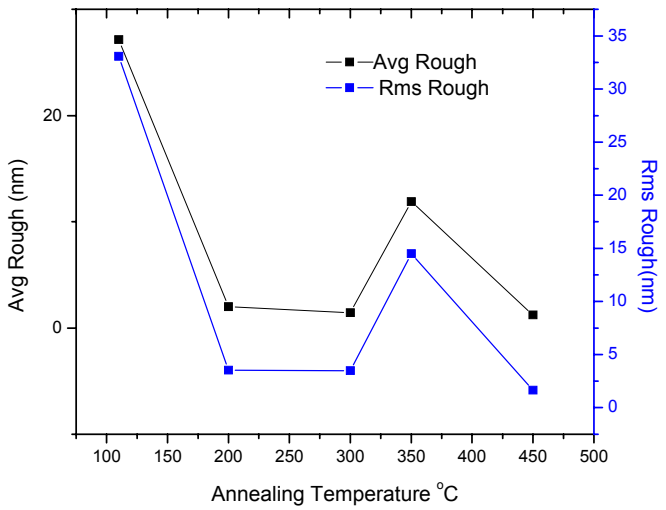

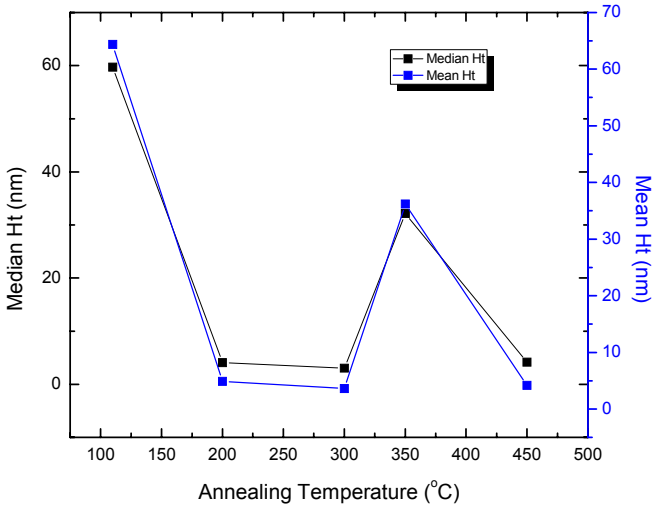

Fig. 8 Variation in (a) AFM images of un-doped zirconia

The above graph shows that there is a systematic decrease in the Ra and Rq value when the temperature increased from 110°C to 200°C and remains stability at the temperature of 300°C. But when temperature increases from 300°C to 350°C the Rq and Ra are again high. The increased roughness on either side can be correlated to changes in the structure of zirconia nanopowder as of function of increased annealing temperature. Effect of annealing temperature on the mean height and median height were also examined and it was found out that as the annealing temparture increased the mean height as well as median height of the samples going to decrease.

Vickers hardness results showed ~564 HV hardness of ZrO_2 samples prepared by sol-gel which is comparable to the hardness values achieved in our sputtered thin films (~ 580 HV) and to the previous work reported by our group (Asghar 2010). It has also observed that there is a positive effect of the accumulation of iron oxide on the fracture toughness and the strength of the ZrO_2 nanoparticles. Improved hardness values of ~ 610 HV was observed in the case of α-Fe_2O_3 doped ZrO_2 nanoparticles which is greater than the value reported earlier (Shon 2011).

CONCLUSIONS

By using sol-gel method the morphology of the prepared zirconia samples, along with the possessions of dopant (Fe_2O_3) has been studied in this work. It could be observed from XRD analysis that tetragonal phase of zirconia has been achieved, which is the required phase of zirconia to use it in different biomedical applications such as in bone implanting, tissue engineering, and oral planting. The SEM images exposed that how the dissimilar morphologies of nanoparticles appeared in un-doped zirconia by variation in the annealing temperature and also by the accumulation of iron oxide. The particles size obtained from SEM micrographs is ~40-50 nm for un-doped zirconia and ~

30- 35nm for doped zirconia. It has been instigated, that in substitutional locations the iron ions softened in stabilized zirconia. AFM images show remarkable decrease in average (27.1 to 1.2 nm) and RMS (33.07 to 1.65 nm) roughness of the samples by the incorporation of organic additives. It is also observed that modification in the zirconia surface can be obtained with the influence of iron into zirconia structure. Positive effect of the accumulation of iron oxide on the fracture toughness and the strength of the zirconia ceramics was observed. Hardness value of ~ 610 HV was observed in the case of iron oxide doped ZrO2 nanoparticles which is larger as compared to the un-doped values (564HV).

REFERENCES

Asghar, M.H., Shoaib, M., Khan, Z.M., Placido, F., Naseem, S., and Mehmood M. (2010), "Complex Optical Filter Prepared by Sputter Deposition." *Eur. Phys. J. Appl. Phys.,* Vol. **49**, 20501-20506.

Ausheliba, M.N., Jagerb, N.D., Kleverlaanb, C.J. and Feilzerb, A.J. (2012) "The Influence of Pigments on the Slow Crack Growth in Dental Zirconia." *Dental materials,* Vol. **28**, 410–415.

Bastide, B. (1989), "Characterization of a new ternary Ce-Y-tetragonal zirconia." Conference proceedings on the Science and Technology of Zirconia, American Ceramic Society.

Boutz, M.M.R., Winnubst, A.J.A., Hartgers, F., Burgraaf, A.J. (1994)," Effect of additives on densification and deformation of tetragonal zirconia." Mater. Sci., Vol. **29**, 5374-5382.

Chevalier, J. and Gremillardw, L. (2009), "The Tetragonal-Monoclinic Transformation in Zirconia: Lessons Learned and Future Trends." *J. Am. Ceram. Soc.*, Vol. **92** [9], 1901–1920.

Chuach, G.K. (1999), "An investigation into the preparation of high surface area zirconia." *Catal. Today*, Vol. **49**(1–3), 131–139.

Chuach, G.K. and Jaenicke, S. (1996), "The influence of preparation conditions on the surface area of zirconia." *Appl. Catal. A.*, Vol. **145**(1–2), 267–284.

Dwivedi, R. Maurya, A. Verma, A. Prasad, R. Bartwal, K.S. (2011), "Microwave assisted sol–gel synthesis of tetragonal zirconia nanoparticles." J. Alloys Compd., Vol. **509**, 6848–6851.

Garcia, F.L. Resende, V.G. Grave.E. Peigney, A. Barnabe, A. Laurent, C. (2009)," Iron-stabilized nanocrystalline ZrO2 solid solutions: Synthesis by combustion and thermal stability." Mater. Res. Bulletin., Vol. **44**, 1301–1311.

Heshmatpour, F. Aghakhanpour, R.B. (2011), "Synthesis and characterization of nanocrystalline zirconia powder by simple sol–gel method with glucose and fructose as organic additives." Powder Tech., Vol. **205**, 193–200.

Jiang, J. Z. Poulsen, F.W. and Mørup, S. (1998), "Structure and thermal stability of nanostructured iron-doped zirconia prepared by high-energy ball milling." J. Mater. Res., Vol. **14**, 4.

Kim, J.D., Hana, S., Kawagoe, S., Sasaki, K. and Hata, T. (2001), "Preparation of perovskite, Pb(Zr, Ti)O_3 thin-films on YSZ(111)/Si(111) substrates by post-deposition annealing." *Thin Solid Films.*, Vol. **385** (5), 293–297.

Kiminami, R.H.G. (1990), "The Monoclinic-Tetragonal Phase Transformation of Zirconia in the System ZrO_2-Fe_2O_3." *J. Mater. Sci.*, Vol. **9**, 373-374.
Laurent, M. Schreiner, U. and Langjahr, P.A. (2001), "Microstructural and electrical characterization of La-doped PZT ceramics prepared by a precursor route." *J. Eur. Ceram. Soc.*, Vol. **21**(10-11), 1495–1498.
Majchrowski, A. Ebothe, J. Gondek, E. Ozga, K. Kityk, I.V. Reshak, A.H. Lukasiewicz, T. (2009), "Photoinduced nonlinear optical effects in the Pr doped BiB3O6 glass nanoparticles incorporated into the polymer matrices." *J. Alloys Compd.*, Vol. **48**, 29–32.
Martinson, A.B.F. Elam, J.W. Hupp, J.T. and Pellin, M.J. (2007), "ZnO Nanotube Based Dye-Sensitized Solar Cells." *Nano Lett.*, Vol. **7**(8), 2183–2187.
Minh, N.Q. (1993), "Elastic properties of ceramic oxides used in solid oxide fuel cells (SOFC)." *J. Am. Ceram. Soc.*, Vol. **76** (3), 563–588.
Manicone, P.F., Lommetti, P.R., Raffaelli, L, (2007) "An overview of zirconia ceramics: Basic properties and clinical applications", J. Dent., 35, 819-826
Ortiz, C. J. L. Rosa, J.R. Ramírez, A.H. Cuellar, E.M.L. Pérez, G.B. Guardiola, R.C.M. Solís, C.D.P. (2010), "La-, Mn- and Fe-doped zirconia catalysts by sol–gel synthesis: TEM characterization, mass-transfer evaluation and kinetic determination in the catalytic combustion of trichloroethylene." Colloids and Surfaces A: chem. phys. Eng. Asp., Vol. **371**, 81–90
Prabakaran, K., Kannan, S. and Rajeswari, S. (2005), "Development and characterisation of zirconia and hydroxyapatite composites for orthopaedic applications." *Trends Biomater. Artif. Organs.*, Vol. **18** (2), 114–116.
Ramalingam, S., Reimanis, I.E., Fuller, E.R. and Haftel, J.D. (2011), "Slow Crack Growth Behavior of Zirconia-Toughened Alumina and Alumina Using the Dynamic Fatigue Indentation Technique." *J. Am. Ceram. Soc.,* **94** (2) 576–583.
Reddy, B.M. and Khan, A. (2005), "Recent Advances on TiO2-ZrO2 Mixed Oxides as Catalysts and Catalyst Supports." *Catal. Rev.*, Vol. **47**(2), 257–296.
Riaz, S., Akbar, A. and Naseem, S., (2012) "Structural, Electrical and Magnetic Properties of Iron Oxide Thin Films" *Adv. Sci. Lett.,* In Press
Shon, I-J., Kang, H-S., Ko, I-Y, Yoon, J-K. and Doh, J-M " Fast Low-Temperature Consolidation of Nnanocrystalline Fe-ZrO_2 Composite by High-Frequency Induction-Heated Sintering", *Rev. Adv. Mater. Sci.* **28** (2011) 1-4
Stefanic, G., Grzeta, B. and Music, S. (2000)," Influence of oxygen on the thermal behavior of the ZrO_2–Fe_2O_3 system." *Mater. Chem. Phys.*, Vol. **65**, 216-221.